

Comparison of G-Protein Coupled Receptor Desensitization-Related β -Arrestin Redistribution Using Confocal and Non-Confocal Imaging

Dorothea Haasen, Michael Wolff, Martin J. Valler and Ralf Heilker*

Boehringer Ingelheim Pharma GmbH & Co. KG, Department of Integrated Lead Discovery, Birkendorfer Str. 65, D-88397 Biberach, Germany

Abstract: High Content Screening (HCS), a combination of fluorescence microscopic imaging and automated image analysis, has become a frequently applied tool to study test compound effects in cellular disease-modelling systems. In this work, we compared a confocal and a non-confocal cellular HCS system, the IN Cell Analyzers¹ 3000TM and 1000TM, respectively. As a cellular model system we used the TransfluoTM 2 technology in the 384-well microtiter plate (MTP) format. The Transfluo HCS assay for G-protein coupled receptor (GPCR) activation is based on the recruitment of a green fluorescent protein-labelled arrestin (ArrGFP) from the cytosol to the plasma membrane. We investigated two GPCRs, the wild-type (wt) β 2 adrenergic receptor (β 2AR) and the β 2AR-enhanced (E), a C-terminally mutated receptor with a higher affinity to arrestin. Upon agonist stimulation, the β 2AR-wt induced the redistribution of ArrGFP to coated pits, the β 2AR-E maintained the interaction with ArrGFP down to the formation of endocytic vesicles. Our findings reveal that the assay is feasible on both instruments, with sufficiently robust Z' statistics. Improved Z' statistics, though, are achieved with the confocal system, particularly in case of weak signals. Moreover, throughput is dramatically higher for the IN Cell Analyzer 3000. We conclude that, depending on the needs for throughput and assay biology, either instrument may fulfil a successful role in the drug discovery process. Confocal optics, however, provide a better basis for the detection of smaller subcellular structures with lower fluorescence intensity.

Keywords: High content screening, confocal imaging, β -arrestin redistribution, subcellular translocation.

INTRODUCTION

Fluorescence microscopy has been widely used in academic cell biology research as a non-destructive and sensitive technique for the visualization of intracellular structures and biomolecular translocations and has benefited substantially from the introduction of confocal microscopy. In a confocal microscopic image, the spatial resolution in the vertical direction is dramatically improved by reducing background fluorescence from above or below the focal plane.

In classic confocal optics [1], this restriction to fluorescence emission from a specific focal plane is achieved by guiding the emitted light through a pinhole (Fig. 1A). However, the available confocal point scanning microscopes, which are based on this optical assembly, are generally too slow for drug screening applications. In contrast, three confocal, high-throughput cellular imagers achieve a throughput that enables their use in an HTS environment [2]: the IN Cell Analyzer 3000 [3] from GE Healthcare Biosciences (Little Chalfont, United Kingdom), the OperaTM [4] from Evotec Technologies GmbH (Hamburg, Germany),

and the BD PathwayTM Bioimager [5] from Becton, Dickinson and Company (USA). To reduce measuring time, the OperaTM and the Pathway HTTM employ a Nipkow disk [6] to project fluorescence from several confocal volumes in parallel to a charged coupled device (CCD) camera, while the IN Cell Analyzer 3000 employs line scanning [3] through a confocal slit (Fig. 1B). The IN Cell Analyzer 3000 offers three laser lines (364 nm, 488 nm, 647 nm) for fluorescence excitation. A 40x Nikon extra-long working distance (ELWD) Plan Fluor/0.6 NA objective provides the combined benefits of a rather large field of view (FOV; 0.56 mm²) with a good optical resolution. Three CCD cameras enable simultaneous confocal imaging at three different emission wavelengths.

The IN Cell Analyzer 1000 [7, 8] is a nonconfocal cellular imaging device based on an inverted epifluorescence microscope (Fig. 1C) with a xenon lamp as the light source. For the comparative studies described below we utilized (a) the standard 10x objective of the IN Cell Analyzer 1000 with a similar field of view (FOV; ~0.6 mm²) as the 40x objective of the IN Cell Analyzer 3000 and (b) the 40x objective of IN Cell Analyzer 1000 with the same optical resolution as the IN Cell Analyzer 3000.

Microscopic imagers as exemplified by the above IN Cell Analyzer 1000 and 3000 have enabled a novel technology platform referred to as "High (Information) Content Screening" (HCS), which has become broadly applied in the pharmaceutical industry [9-11]. In accordance with earlier publications [9, 12, 13], we define HCS as high resolution fluorescence microscopic imaging of fluorophore-labelled

*Address correspondence to this author at the Boehringer Ingelheim Pharma GmbH & Co. KG, Department of Integrated Lead Discovery, Birkendorfer Strasse 65, D-88397 Biberach an der Riss, Germany; Tel: +49-7351-54 5590; Fax: +49-7351-83 5590; E-mail: Ralf.Heilker@bc.boehringer-ingelheim.com

¹IN Cell Analyzer is a trademark of GE Healthcare Bio-Sciences (Little Chalfont, UK); Transfluo is a licensed product of Molecular Devices (Sunnyvale, CA, USA).

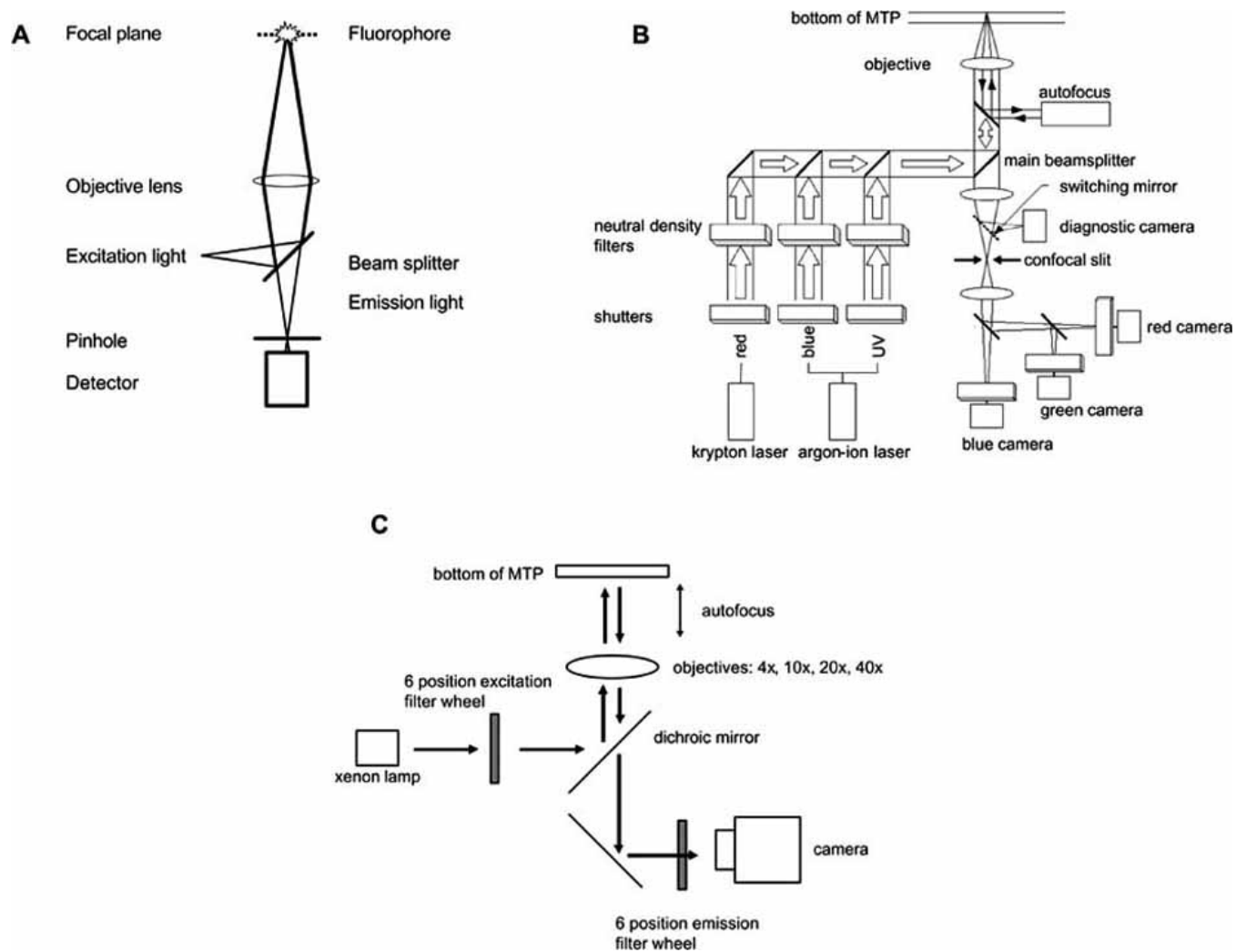


Fig. (1). Confocal optics, optical assemblies of the IN Cell Analyzers 3000 and 1000. **(A)** Confocal optics: The laser excitation light (blue) is focused through the objective to a diffraction-limited point in the focal plane. Only the emitted light (green) from fluorophores in the focal plane passes through the pinhole to the detector. **(B)** The IN Cell Analyzer 3000 employs line scanning through a confocal slit. Two laser lines (364 nm, 488 nm) from an Argon ion laser and one laser line (647 nm) from a Krypton laser are individually guided through neutral density filters. All three laser lines may then be combined. After reflection by a beamsplitter they are auto-focused *via* a 40x Nikon extra-long working distance (ELWD) Plan Fluor/0.6 NA objective to the adherent cell layer in the assay MTP. Emission light is collected through the same objective, then passed through the above beamsplitter and guided through a confocal slit. The light is then split into up to three wavelength ranges, which allows us simultaneous confocal imaging using three 12 bit -35°C cooled CCD cameras. **(C)** The IN Cell Analyzer 1000 is a nonconfocal cellular imaging device based on an inverted epifluorescence microscope. The instrument employs a xenon lamp as the light source, the light is guided through a six-position filter wheel and is then reflected by an appropriate dichroic mirror *via* the objective to the sample. The instrument is compatible with four objectives: 4x/0.2, 10x/0.45, 20x/0.45, 40x/0.6. The emission light is collected through the objective and then passed through the dichroic mirror. After passing through an emission filter (in a six-position filter wheel) the light is detected by a 12 bit -30°C thermoelectrically cooled CCD camera.

cells combined with automated image analysis. Typically, several fluorophores can be observed in parallel (multiplexing). Image analysis software quantifies intracellular translocations of fluorophore-labelled biomolecules. Apart from protein trafficking [10], HCS can provide information on the phosphorylation state of target proteins [14], on cellular

proliferation [15] or apoptosis [16], on morphological changes such as neurite outgrowth [17], on modifications of the cytoskeleton [18, 19], on cellular movements [20] and on other phenomena [11], which result in an overall change of the fluorescence microscopic cellular image.

In this work, we investigated the suitability of the IN Cell Analyzer 3000 and 1000 to measure the Transfluo assay platform, meanwhile a licensed product of Molecular Devices (Sunnyvale, CA, USA). The Transfluo technology is an HCS assay format in which an arrestin-green fluorescent protein (ArrGFP) conjugate redistributes upon GPCR stimulation [21, 22].

The broad applicability of the Transfluo approach is based on the common phenomenon of GPCR “desensitization” and has been demonstrated for numerous GPCRs, independent of the interacting G-protein or of the class of GPCR ligand [21]. Briefly, most GPCRs are desensitized following agonist stimulation [23, 24]. This desensitization is mediated by GPCR kinases (GRKs) and by arrestins (Fig. 2; scheme of GPCR-activation dependent β -arrestin redistribution). GRKs phosphorylate agonist-activated GPCRs on serine and threonine residues. Arrestins are cytoplasmic proteins that are recruited to the plasma membrane by GRK-phosphorylated GPCRs [25]. Arrestins then uncouple the GPCR from the cognate G protein [26, 27], and target the desensitized receptors to clathrin-coated pits for endocytosis [28,29]. If the interaction between arrestin and a GPCR (such as β 2AR) is of low affinity, the arrestin is released after the formation of clathrin-coated pits [30,31]. If the interaction between arrestin and the GPCR (such as vasopressin 2 receptor [V_2R]) is of high affinity, the arrestin is co-internalized with the GPCR to endocytic vesicles.

In the following study, we used paraformaldehyde (PFA)-fixed MTP samples of the wild-type (wt) and a mutant

“enhanced” (E) form of the β 2AR, kindly provided by Xsira Pharmaceuticals (formerly known as Norak Biosciences). The mutant β 2AR-E contains changes in the cytoplasmic C-terminus that increase the affinity of the interaction with arrestin so that arrestin is co-internalized with endocytic vesicles upon receptor activation. We investigated the arrestin redistribution in ArrGFP/ β 2AR-double stable human osteosarcoma (U2OS) cells. The IN Cell Analyzers 3000 and 1000 were employed to record confocal and non-confocal microscopic images of the β 2AR agonist-stimulated ArrGFP/ β 2AR cells. The ArrGFP redistribution to coated pits or endocytic vesicles was quantified using the same image analysis algorithm.

MATERIALS AND METHODS

The construction of the plasmids encoding the human β 2AR-wt/ β 2AR-E and the ArrGFP as well as the establishment of U2OS- β 2AR/ArrGFP double stable cells and the respective cell culture conditions have been described earlier [21, 25, 31, 32].

Quantitative Determination of ArrGFP Redistribution in U2OS- β 2AR/ArrGFP Cells

The cell culture and the bioassay protocols up to PFA fixation were carried out at Xsira Pharmaceuticals: U2OS- β 2AR(-wt or -E)/ArrGFP double stable cells were plated in 384-well glass bottom microtiter plates (MTP; MatriCal, Inc., Spokane, WA) and incubated overnight. For the antagonist dose-inhibition experiments, the wells were pretreated with vehicle or the indicated concentrations of

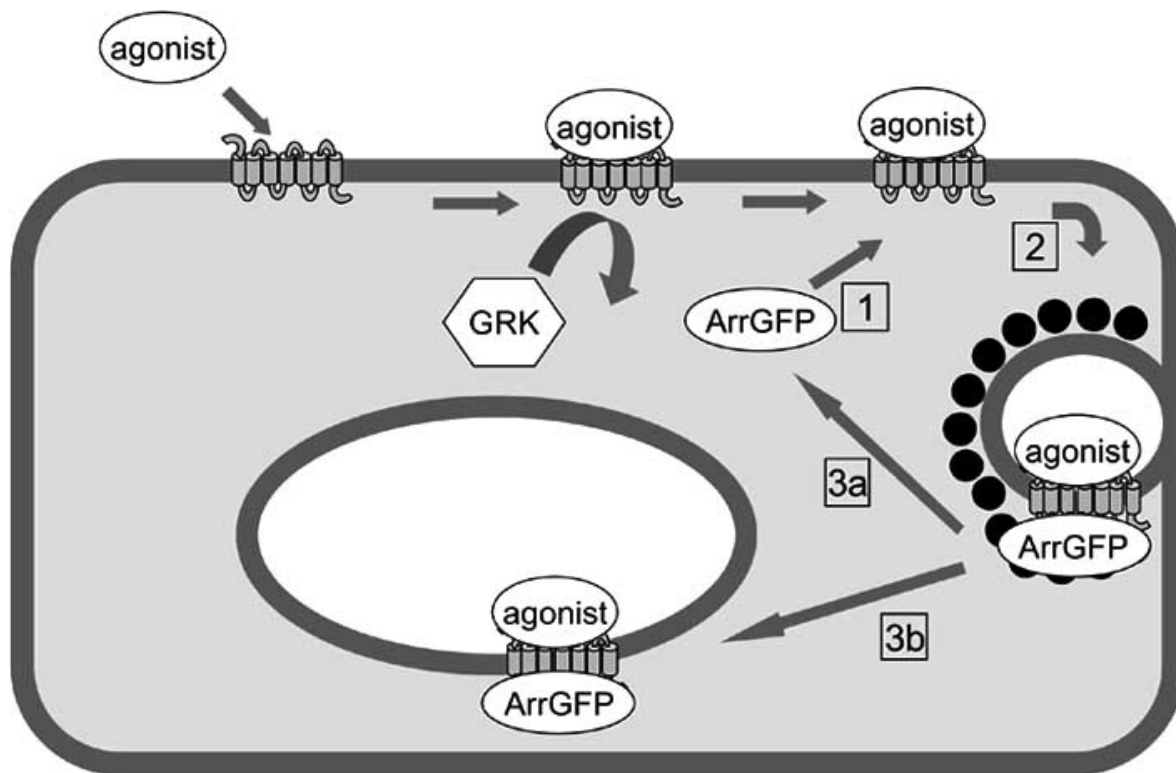


Fig. (2). Model of the Transfluo technology based ArrGFP redistribution. A GRK phosphorylates the agonist-activated GPCR on its carboxy-terminal tail. (1) ArrGFP is recruited to the plasma membrane by the GRK-phosphorylated GPCR. (2) ArrGFP then targets the GPCR to clathrin-coated pits for endocytosis. Depending on the stability of the specific GPCR-arrestin interaction, the ArrGFP is either (3a) released after the formation of clathrin-coated pits or (3b) co-internalized with the GPCR-loaded vesicles.

propranolol for 30 min at 37°C and exposed to 50 nM isoproterenol for an additional 30 min at 37°C. For the agonist dose-response experiments, the wells were directly treated with the indicated concentrations of isoproterenol for 30 min at 37°C. Cells were fixed with 2% PFA and in parallel the cell nuclei were stained with Draq5 dye (2 μM; Biostatus Limited, Shepsted, Leicestershire, UK) for 45 min at room temperature.

The MTPs with the PFA-fixed cellular samples were sent to Boehringer Ingelheim Pharma using a cold pack and then stored at 4° C. At Boehringer Ingelheim Pharma, the MTPs were imaged and analyzed repeatedly using the IN Cell Analyzer 3000 and the IN Cell Analyzer 1000 over the next 1-4 weeks without a detectable change in cellular morphology or fluorescence intensity. The images from the IN Cell Analyzer 1000 were converted by a proprietary software (123™ software; GE Healthcare Biosciences) to the IN Cell Analyzer 3000 image format. The complete image information content is retained upon conversion. For both devices the redistribution of ArrGFP to coated pits for the β2AR-wt and to vesicles for the β2AR-E was quantified using GE granularity analysis module reference GRN0.

Briefly, through the GRN0 algorithm, nuclei are identified as pixel accumulations within a specified area range above a specified intensity threshold in the red (647nm) channel image. In a specified dilated mask region around these nuclei, grains of a pre-specified size and intensity, corresponding to the ArrGFP-stained coated pits or vesicles are identified within the green (488nm) channel image. The GRN0 parameter settings for the size and intensity gradient of the fluorescent grains were individually optimized for IN Cell Analyzer 3000- or 1000-derived images and for images of β2AR-wt or -E cells

The F-grain value is calculated as below:

$$F_{\text{grain}} = \frac{\text{Sum of pixel values in test boxes corresponding to valid grains}}{\text{Sum of pixel values in dilated mask region}} \times 1000$$

An F-grain value of 100 therefore corresponds to 10% of the dilated mask area being represented by valid grains.

Dose-response curves were calculated using GraphPad PRISM Software from GraphPad Software (San Diego, CA 92130 USA).

IN Cell Analyzer 3000

The IN Cell Analyzer 3000 employs line scanning through a confocal slit. Two laser lines (364 nm, 488 nm) from an Argon ion laser and one laser line (647 nm) from a Krypton laser are individually guided through neutral density filters. All three laser lines may then be combined. After reflection by a beamsplitter they are auto-focused *via* a 40x Nikon ELWD Plan Fluor/0.6 NA objective to the adherent cell layer in the assay MTP. Emission light is collected through the same objective, then passed through the above beamsplitter and guided through a confocal slit. The light is split into up to three wavelength ranges, which permits simultaneous confocal imaging using three 12 bit -35°C cooled CCD cameras. For our experiments, we employed the 488 nm laser line (121 mW; attenuated by a neutral density filter to 10%) combined with the 535BP45 emission filter for GFP, and the 647 laser line (49 mW; attenuated by a

neutral density filter to 1%) combined with the 695BP55 emission filter for Draq5™. Fluorescence emission was simultaneously recorded in the green and in the red channel. Prior to the cellular imaging, a flat field correction for inhomogeneous illumination of the scanned area was carried out using an MTP well containing 100 nM Oregon Green™ (Molecular Probes, Inc.; Eugene, OR) and 3 μM Cy5 solution (GE Healthcare Biosciences). For the individual imaging runs, the binning and the area scan widths are indicated below. All measurements were conducted at room temperature.

IN Cell Analyzer 1000

The IN Cell Analyzer 1000 is a nonconfocal cellular imaging device based on an inverted epifluorescence microscope. The instrument employs a xenon lamp as the light source, the light is guided through a six-position filter wheel and is then reflected by an appropriate dichroic mirror *via* the objective to the sample. The instrument is compatible with four objectives: 4x/0.2, 10x/0.45, 20x/0.45, 40x/0.6. The emission light is collected through the same objective and then passed through the dichroic mirror. After passing through an emission filter (one from a six-position wheel) the light is detected by a 12 bit -30°C thermoelectrically cooled CCD camera.

For our experiments, we employed the S475/20X excitation filter combined with the 51008bs dichroic mirror and the HQ535/50M emission filter for GFP. In a subsequent run the HQ620/60X excitation filter was combined with the same 51008bs dichroic mirror and the HQ700/75M emission filter for Draq5™. We used the 10x/0.45 or the 40x/0.6 objective as indicated in the respective experiments. No binning was applied. All measurements were conducted at room temperature.

Statistical Data Analysis

The “high values” correspond to the Fgrain values for the non-inhibited ArrGFP translocation. The “low values” describe the Fgrain values in the absence of a β2AR stimulation.

Z' values were calculated as described previously [33]:

$$Z' = 1 - \frac{3 SD_{\text{high}} + 3 SD_{\text{low}}}{\text{ABS}(\text{Mean}_{\text{high}} - \text{Mean}_{\text{low}})}$$

SD_{high} is the standard deviation of the “high values”, Mean_{high} is the mean value of the “high values”, SD_{low} and Mean_{low} are the respective numbers for the “low values”, ABS(x) is the absolute value of x.

The signal-to-noise (S:N) ratio was calculated as follows:

$$S : N = \frac{\text{ABS}(\text{Mean}_{\text{high}} - \text{Mean}_{\text{low}})}{\sqrt{\text{SD}_{\text{high}}^2 + \text{SD}_{\text{low}}^2}}$$

RESULTS AND DISCUSSION

Z' Statistics of the ArrGFP Redistribution in the 384-Well Format Using the IN Cell Analyzers 3000 and 1000

Fig. 3 shows the results of the image analysis from the isoproterenol-stimulated or mock-treated β2AR-wt/ArrGFP

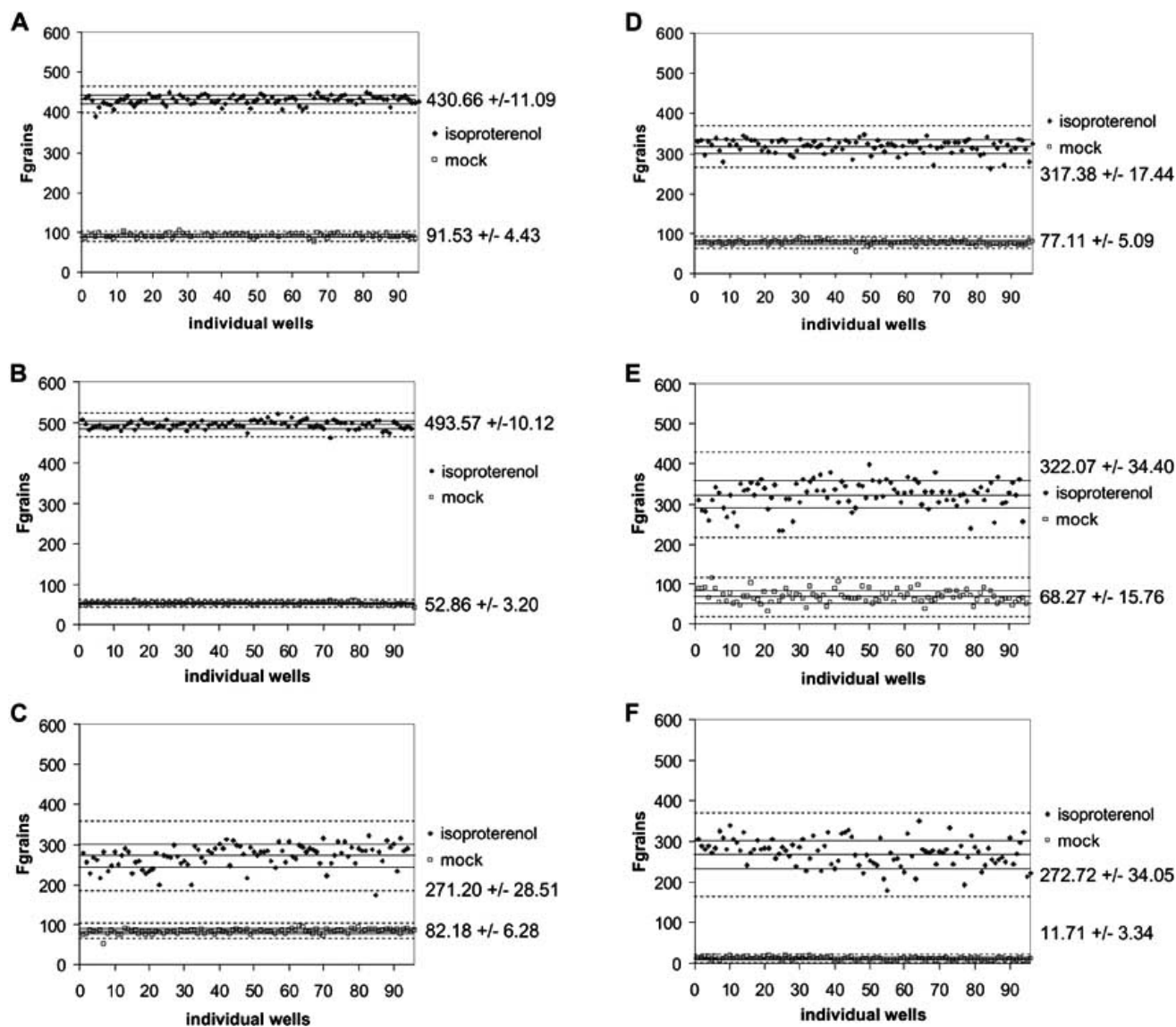


Fig. (3). Statistical analysis of $\beta 2\text{AR}$ (-wt or -E)/ArrGFP double transfected U2OS cells in 384-well MTPs using the IN Cell Analyzer 3000 and 1000 for the measurement. The $\beta 2\text{AR}$ -wt (A/C/E) or -E (B/D/F) transfected cells were stimulated with 1 μM isoproterenol for 30 min at 37°C for the “high” controls (black diamonds; $n > 90$ wells) and mock-treated with vehicle for the “low” controls (open squares; $n > 90$ wells). Cells were fixed with 2% PFA and in parallel the cell nuclei were stained with Draq5 dye (2 μM) for 45 min at room temperature. The MTPs were then analyzed using the IN Cell Analyzer 3000 (A/B) and the IN Cell Analyzer 1000 with the 10x (C/D) as well as the 40x objective (E/F). The images from the IN Cell Analyzer 1000 were converted by the 123 software to the IN Cell Analyzer 3000 data format. The redistribution of ArrGFP to coated pits for the $\beta 2\text{AR}$ -wt and to vesicles for the $\beta 2\text{AR}$ -E was quantified using the granularity analysis module (GRN0). The continuous lines indicate the mean scintillation value for the “high” and the “low” controls. The dotted lines indicate a distance of 1 SD, the dashed lines a distance of 3 SD from these mean values.

and $\beta 2\text{AR}$ -E/ArrGFP double stable U2OS cell lines. Corresponding representative example images (10x or 40x objective) are given in Fig. 4.

The $\beta 2\text{AR}$ -wt belongs to the class of GPCRs that forms low affinity complexes with arrestin. Arrestins were recruited by the $\beta 2\text{AR}$ (wt) from the cytosol to the plasma membrane and then co-localized with $\beta 2\text{AR}$ (wt) to the coated pits but were not further co-internalized in the timeframe of the experiment. Significantly more fluorescence intensity associated with coated pits was identified in the IN Cell Analyzer 3000-derived confocal images of stimulated $\beta 2\text{AR}$ -

wt cells (~430 Fgrains; Fig. 3A) than in the non-confocal images originating from the IN Cell Analyzer 1000, regardless whether the 10x (~270 Fgrains; Fig. 3C) or the 40x (~320 Fgrains; Fig. 3E) objective were employed. Correspondingly, confocal images (exemplified by Fig. 4A/D) (Fig. 3A) produced the best statistical values (Z' of 0.86 and S:N of ~28:1; Table 1). The analysis originating from the non-confocal images (example images in Fig. 4B/E) recorded by the IN Cell Analyzer 1000 using the 10x objective (Fig. 3C) generated significantly inferior assay statistics with a Z' value of 0.45 and a S:N ratio of ~6.5:1.

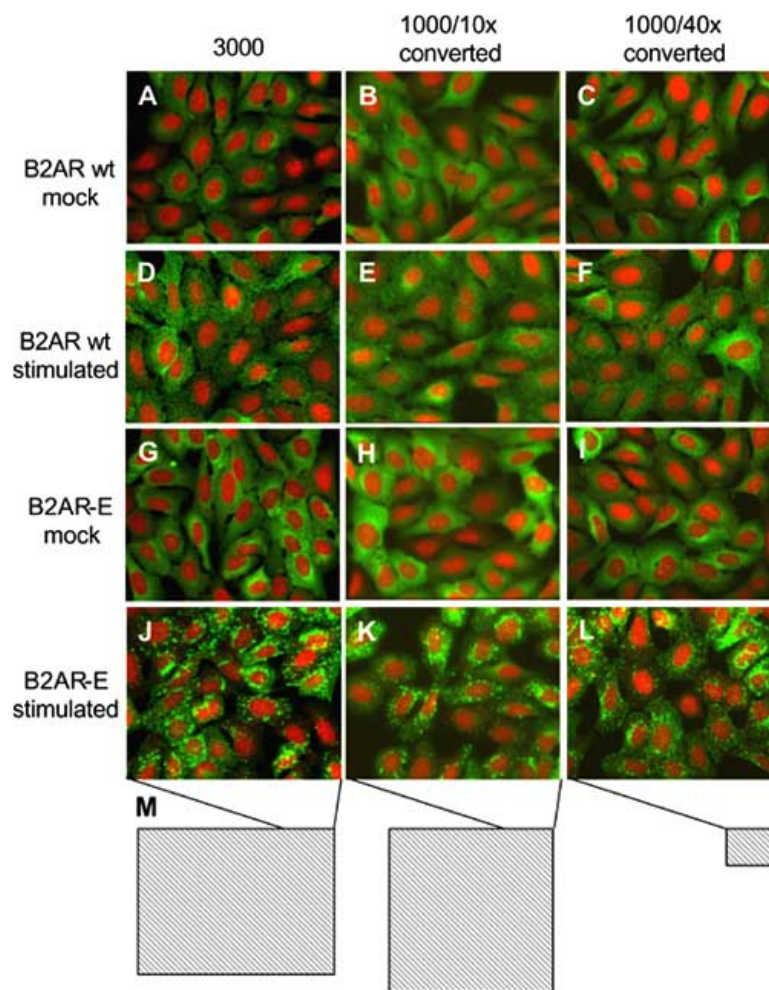


Fig. (4). Distribution of ArrGFP in PFA-fixed U2OS- β 2AR(-wt or -E)/ArrGFP double stable cells. ArrGFP is uniformly distributed in the cytoplasm of mock-treated cells (**A/B/C/G/H/I**). In response to addition of 1 μ M isoproterenol for 30 min at 37°C (**D/E/F/J/K/L**), ArrGFP redistributes either to clathrin-coated pits at the plasma membrane (**D/E/F**) in β 2AR-wt transfected cells or to endocytic vesicles (**J/K/L**) in β 2AR-E transfected cells. Images were recorded using the IN Cell Analyzer 3000 (**A/D/G/J**), or the IN Cell Analyzer 1000 applying the 10x (**B/E/H/K**) and the 40x (**C/F/I/L**) objective. The relative FOVs of the IN Cell Analyzers 3000 and 1000 using the 10x or 40x objective are indicated as hatched areas (**M**) below the respective image columns. The gray areas (**M**) in these FOVs represent the portion of the FOV that is displayed in the above image columns.

When using the 40x instead of the 10x objective in the IN Cell Analyzer 1000, the optical resolution became subjectively better (compare Fig. **4E** and **4F**) but the assay statistics (Z' =0.41, S:N ratio ~6.7:1) were very similar.

In contrast to the wt form, the β 2AR-E mutant binds ArrGFP with a higher affinity so that the arrestin becomes co-internalized to endocytic vesicles. Similar to the analysis of the β 2AR-wt cells, the image analysis of the β 2AR-E cells was much superior when based on the confocal images. Thus, significantly more fluorescence intensity associated with ArrGFP-stained vesicles was identified in the IN Cell Analyzer 3000-derived confocal images (~490 Fgrains; Fig. **3B**) than in the IN Cell Analyzer 1000-derived non-confocal images (~320 Fgrains for the 10x objective and ~270 Fgrains for the 40x objective; Fig. **3D/F**, respectively). Accordingly and similar to the results for the β 2AR-wt cells, the assay statistics for the confocal images of the β 2AR-E cells (Z' of 0.91 and S:N of ~41:1) were notably better than for the corresponding non-confocal images. Comparing the two IN

Cell Analyzer 1000 objectives, the assay statistics were to some extent better for the 10x objective (Z' of 0.72 and S:N of ~13.2:1) than for the 40x objective (Z' of 0.57 and S:N of ~7.6:1).

Overall, the assay statistics of the β 2AR-wt cells are inferior in comparison to those of the β 2AR-E cells. This is most likely because the coated pits in the β 2AR-wt cells appear smaller, dimmer and have a lower background contrast than the vesicles in the β 2AR-E cells. The image analysis for coated pits is therefore more challenging.

It is clear from these results that the non-confocal measurements were inferior to confocal measurements. This is most likely primarily a consequence of the higher background fluorescence and the lower optical resolution of the non-confocal image (compare Fig. **4D** and **4E**). An increased fluorescent background results in fewer grains that fulfil the threshold criteria for a gradient of the grain fluorescence versus the grain surrounding area. In addition,

Table 1. Statistics for the β 2AR-wt and -E Transfluor Assay Using the IN Cell Analyzers 3000 and 1000

Cell line	ArrGFP/ β 2AR-wt			ArrGFP/ β 2AR-E		
Instrument	Z' factor (unstim/stim)	S:N	High/low +/- SD	Z' factor (unstim/stim)	S:N	High/low +/- SD
IN Cell Analyzer 3000	0,86	28,41	H: 430.66 +/- 11.09 L: 91.53 +/- 4.43	0,91	41,52	H: 493.57 +/- 10.12 L: 52.86 +/- 3.20
IN Cell Analyzer 1000 10x objective	0,45	6,48	H: 271.20 +/- 28.51 L: 82.18 +/- 6.28	0,72	13,23	H: 317.38 +/- 17.44 L: 77.11 +/- 5.09
IN Cell Analyzer 1000 40x objective	0,41	6,71	H: 322.07 +/- 34.40 L: 68.27 +/- 15.76	0,57	7,63	H: 272.72 +/- 34.05 L: 11.71 +/- 3.34

we observed some inhomogeneity of illumination in the non-confocal optical system (Fig. 4C/F) which introduced an additional level of heterogeneity to the image analysis for the 40x objective. In contrast to the so-called “flat-field correction” mechanism of the IN Cell Analyzer 3000, correction for non-uniform illumination in the IN Cell Analyzer 1000 is currently not possible.

Agonist Dose Response Curves Based on Images from IN Cell Analyzer 3000 and 1000

Based on the analysis of either confocal or non-confocal images from β 2AR-wt and β 2AR-E cells, dose response curves for the β 2AR agonist isoproterenol were calculated. The cellular samples had been prepared, imaged and quantified as described above. In agreement with the above assay statistical analysis, the GRN0 algorithm detected the highest level of fluorescence intensity associated with coated pits (~400 Fgrains at full isoproterenol stimulation) on the confocal images of stimulated β 2AR-wt cells (Fig. 5A). IN Cell Analyzer 1000-derived non-confocal images of stimulated β 2AR-wt cells displayed less fluorescence intensity associated with coated pits (~350 Fgrains for the 10x objective and ~300 Fgrains for the 40x objective at full isoproterenol stimulation). The calculated EC50 values for isoproterenol were in a narrow range of 2.6-3.7 nM.

In experiments with β 2AR-E cells (Fig. 5B), again more fluorescence intensity associated with ArrGFP-stained vesicles was detected in the confocal images (440 Fgrains at full stimulation) than in the non-confocal images (~330 Fgrains using the 10x objective, ~300 Fgrains using the 40x objective). The isoproterenol EC50 values lay between 3.3 and 4.7 nM, comparable to those of the β 2AR-wt cells, indicating that the ligand binding properties of the β 2AR had not been changed by the C-terminal mutation. Further, the choice of target feature in the image analysis, either coated pit or endocytic vesicle, appeared to have no influence on the observed EC50 values.

We conclude that despite a larger window of Fgrain value measurement from the confocal imager, both the IN Cell Analyzers 3000 and 1000 comparably predict the agonistic potency of a test compound.

Antagonist Dose Inhibition Curves Based on Images from IN Cell Analyzer 3000 and 1000

Based on the analysis of either confocal or non-confocal images from β 2AR-wt and β 2AR-E cells, dose inhibition

curves for the β 2AR antagonist propranolol were calculated. The cellular samples had been prepared, imaged and quantified as described above.

With saturating propranolol concentration the fluorescence intensity associated with coated pits was reduced to the same level of 80-100 Fgrains as for non-stimulated β 2AR-wt cells (compare to Fig. 5A). Analogous to the isoproterenol dose response studies above, the maximal fluorescence intensity associated with coated pits (~400 Fgrains) at low concentrations of propranolol was detected in the confocal images of stimulated β 2AR-wt (Fig. 6A). For the non-confocal images, Fgrain numbers of ~330 for 10x objective and of ~300 for the 40x objective were calculated. Despite the discrepancy between Fgrain values for coated pits derived from confocal and non-confocal images, the propranolol EC50 values were all in a narrow range between 3.4 and 6.2 nM.

The results for the β 2AR-E cells with respect to propranolol inhibition were comparable to those of β 2AR-wt cells. Again higher vesicle numbers were obtained from the confocal than from the non-confocal images at low concentrations of propranolol. The calculated propranolol EC50 values were in the range 4.7 to 5.3 nM, again coincident with the EC50 value span for the β 2AR-wt cells.

In summary, these data suggest that both the IN Cell Analyzer 3000 and 1000 may be used to reliably determine the potency of β 2AR-antagonistic test compounds. However, based on a larger Fgrain window the assay statistics of confocal imaging were found to be superior.

Applicability of the IN Cell Analyzers 3000 and 1000 to High Throughput Screening

The applicability of a cellular imaging device to HTS critically depends on its imaging throughput. Therefore, we compared the MTP imaging time for comparable FOVs in the IN Cell Analyzers 3000 and 1000 (Table 2). The IN Cell Analyzer 3000 required 19 min for measuring all wells of a 384-well MTP when capturing a full image per well. A full image represents an FOV of 0.56 mm² with a pixel resolution of 1280 x 1280 pixel (1.6 Mpixel). Using three CCD cameras in parallel, three independent color images can be recorded simultaneously without impact on the imaging time. The IN Cell Analyzer 1000 images a 384-well MTP at two wavelengths with individual exposure times of 500 ms for the green and 100 ms for the red channel in 33 min. A third color image adds approximately 16 min to the MTP

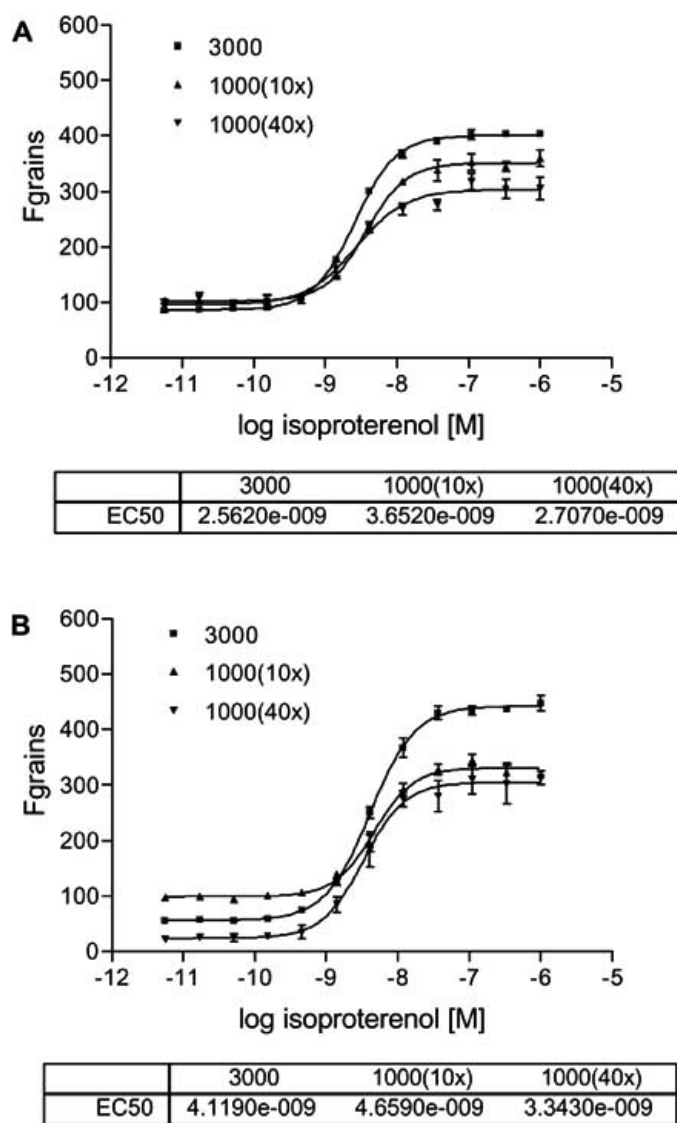


Fig. (5). Isoproterenol dose response curve. The U2OS- β 2AR(-wt or -E)/ArrGFP double stable cells were plated in 384-well MTPs and incubated overnight. Wells were treated with the indicated concentrations of isoproterenol for 30 min at 37°C. Cells were fixed with 2% PFA and in parallel the cell nuclei were stained with DraQ5 dye (2 μ M) for 45 min at room temperature. The MTPs were analyzed in the IN Cell Analyzer 3000 or 1000 (using the 10x or 40x objective) as indicated in the plots. The images from the IN Cell Analyzer 1000 were converted by the 123 software to the IN Cell Analyzer 3000 data format. The redistribution of ArrGFP to coated pits for the β 2AR-wt (**A**) and to vesicles for the β 2AR-E (**B**) was quantified using the granularity analysis module (GRN0). Values are plotted as means of 4 experiments \pm SD. Dose-response curves and EC50 values were calculated using GraphPad PRISM Software.

measurement time. Using the 10x objective, an image covers a FOV of 0.60 mm² and is resolved into 1392 x 1040 pixel (1.4 Mpixel). Using the 40x objective, the FOV is only 0.037 mm². To image approximately the same FOV as with the 10x objective, 16 images of one well using the 40x objective must be captured which extends the imaging time for a 384-well MTP to 530 min.

Some optimisation of image handling is possible. Due to the excellent assay statistics for the Transfluor assay in the IN Cell Analyzer 3000, the imaging area may be reduced by half (i.e. 0.28 mm² or 0.8 Mpixel), or for the full image area 2x pixel-binning may be applied. In pixel-binning, intensity values for adjacent pixels in the sensor array are averaged to generate a lower resolution image, in this case 640 x 640

effective pixels. Either of these techniques reduced the imaging time to ~12 min per 384-well MTP. For the half height imaging, only a minor loss of statistical data quality (for the β 2AR-wt: Z' of 0.83 for the half-height image instead of 0.86 for the full image; for the β 2AR-E: Z' of 0.89 for the half-height image instead of 0.91 for the full image, data not shown). Similarly, the Z' value of 0.91 for the 2x pixel-binning remains unchanged in comparison to the non-binned data with respect to the β 2AR-E (data not shown). When however 2x pixel-binning was applied to the β 2AR-wt data, the Z' value of 0.64 was significantly lower than the respective Z' of 0.86 for the non-binned data. This corresponds to the fact that the coated pit areas detected for the β 2AR-wt are significantly smaller than the vesicles detected for the β 2AR-E. Consequently, the optical

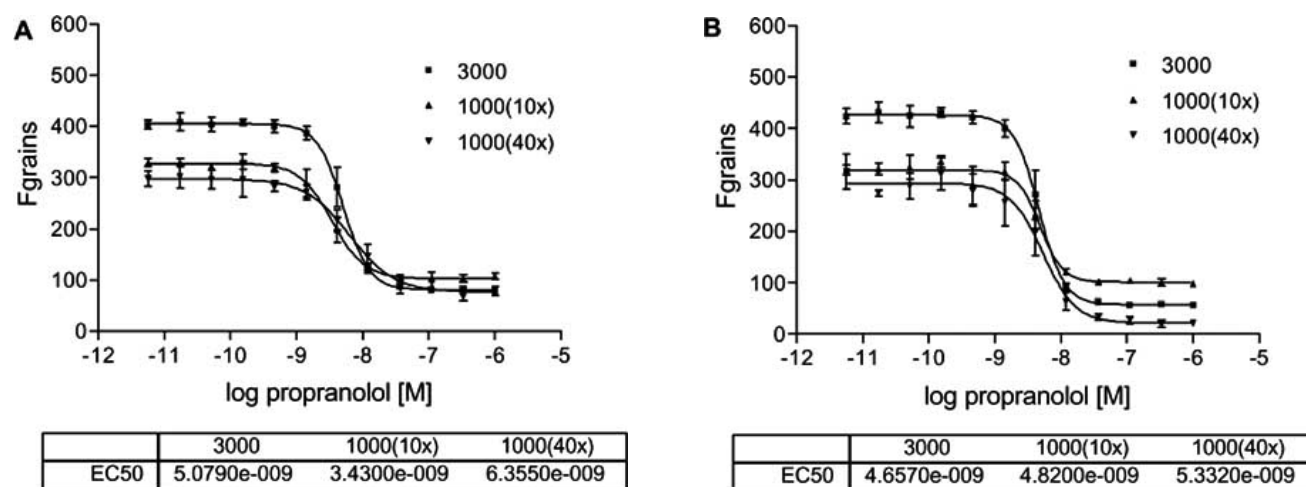


Fig. (6). Propranolol dose inhibition curve. The U2OS- β 2AR(-wt or -E)/ArrGFP double stable cells were plated in 384-well MTPs and incubated overnight. Wells were treated with the indicated concentrations of propranolol for 30 min at 37°C and then exposed to 50 nM isoproterenol for an additional 30 min at 37°C. Cells were fixed with 2% PFA and in parallel the cell nuclei were stained with Draq5 dye (2 μ M) for 45 min at room temperature. The MTPs were analyzed in the IN Cell Analyzer 3000 or 1000 (using the 10x or 40x objective) as indicated in the plots. The images from the IN Cell Analyzer 1000 were converted by the 123 software to the IN Cell Analyzer 3000 format. The redistribution of ArrGFP coated pits for the β 2AR-wt (A) and to vesicles for the β 2AR-E (B) was quantified using the granularity analysis module (GRN0). Values are plotted as means of 4 experiments \pm SD. Dose-response curves and EC50 values were calculated using GraphPad PRISMTM Software.

resolution is more important for the β 2AR-wt. As an estimation of throughput of the IN Cell Analyzer 3000 in a typical automated liquid handling environment, switching between MTPs takes approximately 1 min so that in total half area imaging would require about ~13 min per 384-well MTP, giving eighty-three 384-well MTPs or ~32,000 datapoints per 18 hour day.

The throughput of the IN Cell Analyzer 1000 is evidently lower: with an MTP-to-MTP switching time of about 2 min and an imaging time of 33 min using the 10x objective a throughput of 35 min per 384-well MTP can be calculated. Assuming the same 18 h of continuous imaging per day for an integrated imager, a throughput of about thirty-one 384-well MTPs or ~12,000 datapoints per day can be estimated.

HTS based on cellular imaging generates large data volumes in comparison to conventional screening based on a single numerical measurement per MTP well. Thus, the IN

Cell Analyzer 3000 typically generates a two-color image of about 5.2 MB from one MTP well. Comparably, the IN Cell Analyzer 1000 produces two individual one-color images of about 2.9 MB, together adding up to 5.8 MB per measurement, similar to the IN Cell Analyzer 3000. The IN Cell Analyzer 3000 software, however, allows us the adjustment of image color display and color balance corresponding to emission signals in the two data channels in a single image. In contrast, the IN Cell Analyzer 1000 software generates an additional image with a fixed color balance to visualize an overlay of two emission signals, requiring a further ~4.1 MB of data storage space.

If extrapolated to the measurement of a complete 384-well MTP, both the IN Cell Analyzer 3000 and 1000 generate about 2 GB of image data (Table 2). By using either a “half area” image or 2x binning in the IN Cell Analyzer 3000 as described above, the required data storage volume for a 384-well MTP declines to 1 or 0.5 GB, respectively.

Table 2. Throughput and Characteristics of the IN Cell Analyzers 3000 and 1000

	Area	96-Well format	384-Well format	Field of view [mm ²]	Throughput 384-well MTP in 12h	Storage capacity per 384-well MTP**
IN Cell Analyzer 1000, 10x or 40x objective	1 tile, 10x	8 min	33 min	0.603	20	2.2 (3,8) GB
	1 tile, 40x	8 min	33 min	0.037	20	2.2 (3,8) GB
	16 tiles, 40x	128 min*	530 min*	0.592	1.4*	35.2 (60.8) GB*
IN Cell Analyzer 3000, 40xELWD objective	full image	5 min	19 min	0.563	37	2 GB
	half image	3 min	12 min	0.281	58	1 GB
	2xbinning	3 min	12 min	0.563	58	0,6 GB

*estimated.

**calculation in brackets include overlay images for IN Cell Analyzer 1000.

Data volume reduction becomes particularly relevant at higher MTP throughputs, which may easily raise the annual data storage requirements into the Terabyte range.

CONCLUSIONS

Confocal optics confer a significantly improved spatial resolution for fluorescence microscopy as a tool to investigate test compound effects in disease-modelling cellular systems but typically at the expense of an increased imaging time in comparison to standard epifluorescence microscopes. Novel HTS-compatible, confocal cellular imaging devices achieve an increased throughput by Nipkow-disk based multipoint scanning or by line scanning. In this work, we have investigated a line scanning-based confocal imager, the IN Cell Analyzer 3000, in comparison to a non-confocal imaging device, the IN Cell Analyzer 1000 using the Transflour technology, a well established and robust HCS assay format.

In our studies, we employed the β 2AR-wt as a representative of the low affinity arrestin binder class and a C-terminally mutated β 2AR-E to represent receptors for which arrestin is co-internalized to endocytic compartments. Endocytic vesicles labelled with ArrGFP are larger in size than coated pits and provide a higher fluorescence intensity. The generally superior assay statistics for our studies on the β 2AR-E compared to the β 2AR-wt are in agreement with the hypothesis that the large, bright, high-contrast endocytic vesicles produced with the β 2AR-E are more easily detected and quantified than the small, dim, low-contrast granules generated with the β 2AR-wt. Thus, both the IN Cell Analyzer 3000 and 1000 produce Z' values above 0.5 (a frequently employed threshold for a robust screening assay) for the β 2AR-E related assay. On the contrary, there is a larger difference between the IN Cell Analyzer 3000 (Z' of 0.86) and 1000 (Z' of 0.45) with respect to the β 2AR-wt based Transflour assay. We have shown that the higher quality of the IN Cell Analyzer 3000 images derived from the confocal optics since the comparably reduced quality of the IN Cell Analyzer 1000 could not be overcome by gathering data at an equivalent resolution using a 40x objective.

The two Transflour receptor types, the “coated-pit formers” (with smaller, less fluorescently bright objects) and the “vesicle formers” (with larger, more fluorescently bright objects), are the two major GPCR subclasses distinguished by the Transflour biology. Other GPCRs co-expressed in arrestin-GFP transfected cells can be expected to produce similarly large and fluorescently bright coated pits or vesicles to β 2AR-wt or β 2AR-E, respectively, depending on their arrestin affinity and their corresponding Transflour subclass categorization. Therefore, we think that our experiments enable us to extrapolate imaging results for other GPCR representatives of these two Transflour “subclasses”.

The throughput of the line scanning-based confocal imager, the IN Cell Analyzer 3000, was substantially higher for this application in comparison to the non-confocal imaging device, the IN Cell Analyzer 1000. The imaging time increased dramatically when the two devices were compared on the basis of identical imaged area, i.e. using a

40x objective in the IN Cell Analyzer 1000 to cover a similar area of the MTP well bottom.

Based on the superior image quality, the throughput of the IN Cell Analyzer 3000 may further be increased by, for example, halving the scanned area without a significant loss of quality.

The decision whether to employ a confocal or non-confocal device in an HTS environment will depend on individual throughput and assay biology requirements.

There are certainly some fluorophores, where the use of a white-light source (e.g. Xenon lamp) for fluorescence excitation with exchangeable excitation filters (as available for the IN Cell Analyzer 1000) is advantageous compared to the three fixed excitation laser wavelengths of the IN Cell Analyzer 3000. However, in all our experiments conducted so far, we found the high power of the three IN Cell Analyzer 3000 lasers sufficient also to excite fluorophores with excitation maxima in between these three laser lines.

Further, there are specific biological applications (e.g. an angiogenesis assay across a three-dimensional matrix), where the confocal exclusion of fluorescence emission from above and below the focal layer is disadvantageous in comparison to non-confocal optics. Most assays formats that we looked at so far, however, profited from the increased optical resolution and from the exclusion of background fluorescence provided by the confocal IN Cell Analyzer 3000.

There are certainly limitations to the transferability of our experimental results using the IN Cell Analyzers 3000 and 1000 to other confocal and non-confocal imaging devices and to other assay formats. However, our results suggest that challenging assay biologies with an intrinsically inferior signal-to-noise ratio and the need for HTS compatible throughputs are likely to benefit from fast confocal imaging technologies. As the aims of early drug discovery become increasingly ambitious, we predict a substantially increased use of HCS based on confocal cellular imaging in the near future.

ACKNOWLEDGEMENTS

We thank Xsira Pharmaceuticals Inc. (formerly Norak Biosciences Inc.) for preparing all the paraformaldehyde-fixed biological samples that were used in the above described experiments.

REFERENCES

- [1] Wilson, T. *Confocal microscopy*; Academic Press: **1990**.
- [2] Zemanova, L.; Schenk, A.; Valler, M.J.; Nienhaus, G.U.; Heilker, R. *Drug Discov. Today*, **2003**, 8(23), 1085-1093.
- [3] Glaser, V. *Assay Drug Dev. Technol.*, **2004**, 1(3), 403-408.
- [4] Eggeling, C.; Brand, L.; Ullmann, D.; Jager, S. *Drug Discov. Today*, **2003**, 8, 632-641.
- [5] Vanek, P.G.; Tunon, P. *Gen. Eng. News*, **2002**, 22(13), 1-4.
- [6] Nakano, A. *Cell Struct. Funct.*, **2002**, 27, 349-355.
- [7] Roquemore, L. *Drug Plus International*, **2003**, 2(4), 12-14.
- [8] Amersham Biosciences *IN Cell Analyzer 1000 product pamphlet*, **2003**.
- [9] Ghosh, R.N.; Chen, Y.T.; DeBiasio, R.; DeBiasio, R.L.; Conway, B.R.; Minor, L.K.; Demarest, K.T. *Biotechniques*, **2000**, 29, 170-175.
- [10] Almholt, D.L.; Loechel, F.; Nielsen, S.J.; Krog-Jensen, C.; Terry, R.; Bjorn, S.P.; Pedersen, H.C.; Praestegaard, M.; Moller, S.

- Heide, M.; Pagliaro, L.; Mason, A.J.; Butcher, S.; Dahl, S.W. *Assay Drug Dev. Technol.*, **2004**, *2*, 7-20.
- [11] Li, Z.; Yan, Y.; Powers, E.A.; Ying, X.; Janjua, K.; Garyantes, T.; Baron, B. *J. Biomol. Screen.*, **2003**, *8*, 489-499.
- [12] Conway, B.R.; Minor, L.K.; Xu, J.Z.; Gunnet, J.W.; DeBiasio, R.; D'Andrea, M.R.; Rubin, R.; DeBiasio, R.; Giuliano, K.; DeBiasio, L.; Demarest, K.T. *J. Biomol. Screen.*, **1999**, *4*, 75-86.
- [13] Taylor, D.L.; Woo, E.S.; Giuliano, K.A. *Curr. Opin. Biotechnol.*, **2001**, *12*, 75-81.
- [14] Russello, S.V. *Assay Drug Dev. Technol.*, **2004**, *2*, 225-235.
- [15] Bhawe, K.M.; Blake, R.A.; Clary, D.O.; Flanagan, P.M. *J. Biomol. Screen.*, **2004**, *9*, 216-222.
- [16] Steff, A.M.; Fortin, M.; Arguin, C.; Hugo, P. *Cytometry*, **2001**, *45*, 237-243.
- [17] Simpson, P.B.; Bacha, J.I.; Palfreyman, E.L.; Woollacott, A.J.; McKernan, R.M.; Kerby, J. *Anal. Biochem.*, **2001**, *298*, 163-169.
- [18] Giuliano, K.A. *J. Biomol. Screen.*, **2003**, *8*, 125-135.
- [19] Olson, K.R.; Olmsted, J.B. *Methods Enzymol.*, **1999**, *302*, 103-120.
- [20] Soll, D.R.; Voss, E.; Johnson, O.; Wessels, D. *Scanning*, **2000**, *22*, 249-257.
- [21] Oakley, R.H.; Hudson, C.C.; Cruickshank, R.D.; Meyers, D.M.; Payne, R.E.; Rhem, S.M.; Loomis, C.R. *Assay Drug Dev. Technol.*, **2002**, *1*(1), 21-30.
- [22] Milligan, G. *Drug Discov Today*, **2003**, *8*(13), 579-585.
- [23] Ferguson, S.S. *Pharmacol. Rev.*, **2001**, *53*, 1-24.
- [24] Krupnick, J.G.; Benovic, J.L. *Annu. Rev. Pharmacol. Toxicol.*, **1998**, *38*, 289-319.
- [25] Barak, L.S.; Ferguson, S.S.; Zhang, J.; Caron, M.G. *J. Biol. Chem.*, **1997**, *272*, 27497-27500.
- [26] Lohse, M.J.; Andexinger, S.; Pitcher, J.; Trukawinski, S.; Codina, J.; Faure, J.P.; Caron, M.G.; Lefkowitz, R.J. *J. Biol. Chem.*, **1992**, *267*, 8558-8564.
- [27] Pippig, S.; Andexinger, S.; Daniel, K.; Puzicha, M.; Caron, M.G.; Lefkowitz, R.J.; Lohse, M.J. *J. Biol. Chem.*, **1993**, *268*, 3201-3208.
- [28] Goodman, O.B., Jr.; Krupnick, J.G.; Santini, F.; Gurevich, V.V.; Penn, R.B.; Gagnon, A.W.; Keen, J.H.; Benovic, J.L. *Nature*, **1996**, *383*, 447-450.
- [29] Laporte, S.A.; Oakley, R.H.; Holt, J.A.; Barak, L.S.; Caron, M.G. *J. Biol. Chem.*, **2000**, *275*, 23120-23126.
- [30] Oakley, R.H.; Laporte, S.A.; Holt, J.A.; Caron, M.G.; Barak, L.S. *J. Biol. Chem.*, **2000**, *275*, 17201-17210.
- [31] Oakley, R.H.; Laporte, S.A.; Holt, J.A.; Barak, L.S.; Caron, M.G. *J. Biol. Chem.*, **2001**, *276*, 19452-19460.
- [32] Oakley, R.H.; Laporte, S.A.; Holt, J.A.; Barak, L.S.; Caron, M.G. *J. Biol. Chem.*, **1999**, *274*, 32248-32257.
- [33] Zhang, J.H.; Chung, T.D.; Oldenburg, K.R. *J. Biomol. Screen.*, **1999**, *4*, 67-73.

Received: July 28, 2005

Revised: September 28, 2005

Accepted: November 8, 2005